



HAL
open science

Optical and microstructural properties versus indium content in $\text{In}_x\text{Ga}_{1-x}\text{N}$ films grown by metal organic chemical vapor deposition

Anisha Gokarna, Aurélien Gauthier-Brun, Will Liu, Ydir Androussi, Eric Dumont, El Hadj Dogheche, J.H. Teng, Soojin Chua, Didier Decoster

► **To cite this version:**

Anisha Gokarna, Aurélien Gauthier-Brun, Will Liu, Ydir Androussi, Eric Dumont, et al.. Optical and microstructural properties versus indium content in $\text{In}_x\text{Ga}_{1-x}\text{N}$ films grown by metal organic chemical vapor deposition. *Applied Physics Letters*, 2010, 96 (19), pp.191909. 10.1063/1.3425761 . hal-00549024

HAL Id: hal-00549024

<https://hal.science/hal-00549024v1>

Submitted on 30 May 2022

HAL is a multi-disciplinary open access archive for the deposit and dissemination of scientific research documents, whether they are published or not. The documents may come from teaching and research institutions in France or abroad, or from public or private research centers.

L'archive ouverte pluridisciplinaire **HAL**, est destinée au dépôt et à la diffusion de documents scientifiques de niveau recherche, publiés ou non, émanant des établissements d'enseignement et de recherche français ou étrangers, des laboratoires publics ou privés.

Optical and microstructural properties versus indium content in $\text{In}_x\text{Ga}_{1-x}\text{N}$ films grown by metal organic chemical vapor deposition

Cite as: Appl. Phys. Lett. **96**, 191909 (2010); <https://doi.org/10.1063/1.3425761>

Submitted: 14 December 2009 • Accepted: 07 April 2010 • Published Online: 13 May 2010

A. Gokarna, A. Gauthier-Brun, W. Liu, et al.



View Online



Export Citation

ARTICLES YOU MAY BE INTERESTED IN

[Properties of \$\text{In}_x\text{Ga}_{1-x}\text{N}\$ films in terahertz range](#)

Applied Physics Letters **100**, 071913 (2012); <https://doi.org/10.1063/1.3684836>

[Optical constants of epitaxial AlGaIn films and their temperature dependence](#)

Journal of Applied Physics **82**, 5090 (1997); <https://doi.org/10.1063/1.366309>

[Refractive index of InGaN/GaN quantum well](#)

Journal of Applied Physics **84**, 6312 (1998); <https://doi.org/10.1063/1.368954>

Lock-in Amplifiers
up to 600 MHz



Zurich
Instruments



Optical and microstructural properties versus indium content in $\text{In}_x\text{Ga}_{1-x}\text{N}$ films grown by metal organic chemical vapor deposition

A. Gokarna,^{1,a)} A. Gauthier-Brun,^{1,2} W. Liu,² Y. Androussi,^{1,b)} E. Dumont,³ E. Dogheche,¹ J. H. Teng,² S. J. Chua,² and D. Decoster¹

¹*Institute of Electronics, Microelectronics and Nanotechnology, UMR-8520, Avenue Poincaré, 59652 Villeneuve d'Ascq, Cedex, France*

²*Institute of Materials Research and Engineering (IMRE), Agency for Science, Technology and Research,*

³*Research Link, Singapore 117602*

³*Energy Research Centre, University of Mons, 7000 Mons, Belgium*

(Received 14 December 2009; accepted 7 April 2010; published online 13 May 2010)

We present comparative investigations of single phase $\text{In}_x\text{Ga}_{1-x}\text{N}$ alloys for a varying In content ($x=0.07$ to 0.14) grown by metal organic chemical vapor deposition (MOCVD) technique. While the composition was determined using secondary ion mass spectroscopy, we have investigated the microstructures in $\text{In}_x\text{Ga}_{1-x}\text{N}/\text{GaN}$ films by using transmission electron microscopy and correlated these with the refractive index of the material. Based on ellipsometric analysis of the films, the dispersion of optical indices for $\text{In}_x\text{Ga}_{1-x}\text{N}$ films is determined by using Tauc–Lorentz dispersion equations. © 2010 American Institute of Physics. [doi:10.1063/1.3425761]

$\text{In}_x\text{Ga}_{1-x}\text{N}$ material is a promising ternary alloy system for many optoelectronics applications^{1,2} since its band gap can be tuned from the near infrared region of ~ 0.7 eV (InN) to the near UV region of ~ 3.4 eV (GaN).^{3,4} Recently, high quality In-rich $\text{In}_x\text{Ga}_{1-x}\text{N}$ alloys also offer potential applications in many areas including solar cells,⁴ photoelectrochemical cells,^{5,6} and laser diodes in the wavelength range from blue to green.^{7,8} Growth of $\text{In}_x\text{Ga}_{1-x}\text{N}$ has proved to be extremely challenging due to the large difference in the lattice constant and the difference in the optimum growth temperature of GaN and InN. The big difference in the covalent radii of In and Ga tends to create a large internal strain or causes phase separation thereby resulting in inhomogeneous properties in high In content $\text{In}_x\text{Ga}_{1-x}\text{N}$ films. From high performance device application point of view, a detailed knowledge of key fundamental properties, e.g., dispersion of the refractive index, carrier dynamics, photoluminescence, etc., of $\text{In}_x\text{Ga}_{1-x}\text{N}$ materials is crucial. In literature, Anani *et al.*⁹ have theoretically determined the index dispersion from the band gap calculation, showing a hyperbola tendency for a wide indium content. Sanford *et al.*¹⁰ have also reported the refractive index evolution of $\text{In}_x\text{Ga}_{1-x}\text{N}$ samples for a narrow range of In content ($x=0$ to 0.07). Goldhan *et al.*¹¹ have used a parametric dielectric function model for obtaining refractive index and extinction coefficient for two cubic $\text{In}_x\text{Ga}_{1-x}\text{N}$ samples with In content $x=0.02$ and 0.07 , respectively. However, there is no experimental data until now for $\text{In}_x\text{Ga}_{1-x}\text{N}$ with In composition higher than 0.07 .

In this letter, we report our experimental study of GaN and three types of $\text{In}_x\text{Ga}_{1-x}\text{N}$ samples fabricated with varying In composition, namely, $\text{In}_{0.07}\text{Ga}_{0.93}\text{N}$, $\text{In}_{0.10}\text{Ga}_{0.90}\text{N}$, and $\text{In}_{0.14}\text{Ga}_{0.86}\text{N}$. Structural and optical analysis of these samples grown on sapphire substrates were conducted by x-ray diffraction (XRD), secondary ion mass spectroscopy (SIMS), atomic force microscope (AFM), transmission electron microscopy (TEM), scanning electron microscopy

(SEM), and spectroscopic ellipsometry (SE). The aim of this work is to establish experimentally the values of refractive index for $\text{In}_x\text{Ga}_{1-x}\text{N}$ with In composition higher than 0.07 and to establish a correlation between the microstructure and the optical properties of $\text{In}_x\text{Ga}_{1-x}\text{N}$ which will prove to be highly useful from device application point of view.

$\text{In}_x\text{Ga}_{1-x}\text{N}$ alloys of thickness 200 nm with different In content were grown on GaN (0001)/c-plane Al_2O_3 (sapphire) templates by metal organic chemical vapor deposition (MOCVD). The precursors utilized were trimethylgallium, trimethylindium, and ammonia for Ga, In, and N, respectively. First, a thin (~ 40 nm) GaN seed layer was grown on a sapphire substrate at low temperature (~ 530 °C) followed by high temperature (~ 1050 °C) growth of GaN layer with a thickness of ~ 2.2 μm .¹² Three $\text{In}_x\text{Ga}_{1-x}\text{N}$ samples with varying In composition were then grown on the GaN layer by varying the growth temperature. The growth rate is 140 nm/h, and V/III ratio is 6587 . The thicknesses were determined by SEM.

The In and Ga atomic fractions were determined using SIMS. Since no reference sample was available for such material, the $\text{In}_{0.10}\text{Ga}_{0.90}\text{N}$ indium fraction was determined using Rutherford backscattering spectrometry and the other samples were characterized relatively to this reference value using a TOFSIMS IV from ION-TOF GmbH. Sputtering was done with an Ar^+ 3 kV gun on a 300×300 μm^2 raster area while secondary Ga^+ 25 kV beam was used to analyze a 150×150 μm^2 surface. Figure 1 shows the depth profiles for the three samples inside the $\text{In}_x\text{Ga}_{1-x}\text{N}$ layer. While the In fraction is constant with depth for $\text{In}_{0.07}\text{Ga}_{0.93}\text{N}$, it appears that it varies slightly for $\text{In}_{0.10}\text{Ga}_{0.90}\text{N}$ (up to 0.01 of In) and more broadly for $\text{In}_{0.14}\text{Ga}_{0.86}\text{N}$ (a few percent). The $x=0.14$ fraction was chosen as a mean value but the composition actually varies with the depth in the $\text{In}_x\text{Ga}_{1-x}\text{N}$ layer between $x=0.12$ and $x=0.15$. The thickness of the deposited layers was measured by cross sectional SEM. TEM studies were performed with a Philips CM30 microscope operated at 300 kV. Cross-sectional thin foils were prepared by focused ion beam (FIB) milling technique. For optical investigations, we

^{a)}Electronic mail: anisha.gokarna@iemn.univ-lille1.fr.

^{b)}LSPES, UMR-CNRS 8008, 59950 Villeneuve d'Ascq, France.

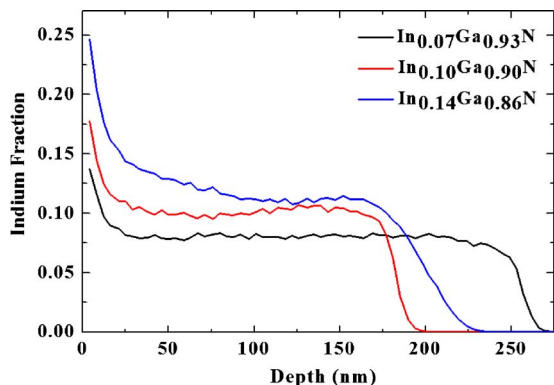


FIG. 1. (Color online) SIMS data of $\text{In}_{0.07}\text{Ga}_{0.93}\text{N}$, $\text{In}_{0.10}\text{Ga}_{0.90}\text{N}$, and $\text{In}_{0.14}\text{Ga}_{0.86}\text{N}$ films grown on GaN/sapphire.

used a spectroscopic ellipsometer (Model UVISEL-NIR from Jobin Yvon). The measurements were performed at an angle of incidence 60° for several photon energies ranging from 0.75 to 4 eV with a step of 0.01 eV for both the GaN/ Al_2O_3 and $\text{In}_x\text{Ga}_{1-x}\text{N}$ /GaN/ Al_2O_3 samples.

TEM analysis was conducted in order to study the microstructural defects present in the layers. Figures 2(a)–2(c) show a weak beam TEM image of $\text{In}_{0.07}\text{Ga}_{0.93}\text{N}$, $\text{In}_{0.10}\text{Ga}_{0.90}\text{N}$, and $\text{In}_{0.14}\text{Ga}_{0.86}\text{N}$, respectively. Threading dislocations are seen to originate in the GaN layer and they extend further into InGaN layer with some of these defects eventually terminating into inverted pyramidal pits (V-pits). The threading dislocations observed in these images maybe either mixed or pure screw type dislocations as the images are taken along $g=0002$ diffraction vector.¹³ The edge dislocations are out of contrast as $gb=0$ (b is burgers vector). From TEM images we can see that the number of V-pits in $\text{In}_{0.10}\text{Ga}_{0.90}\text{N}$ is twice compared to $\text{In}_{0.07}\text{Ga}_{0.93}\text{N}$.

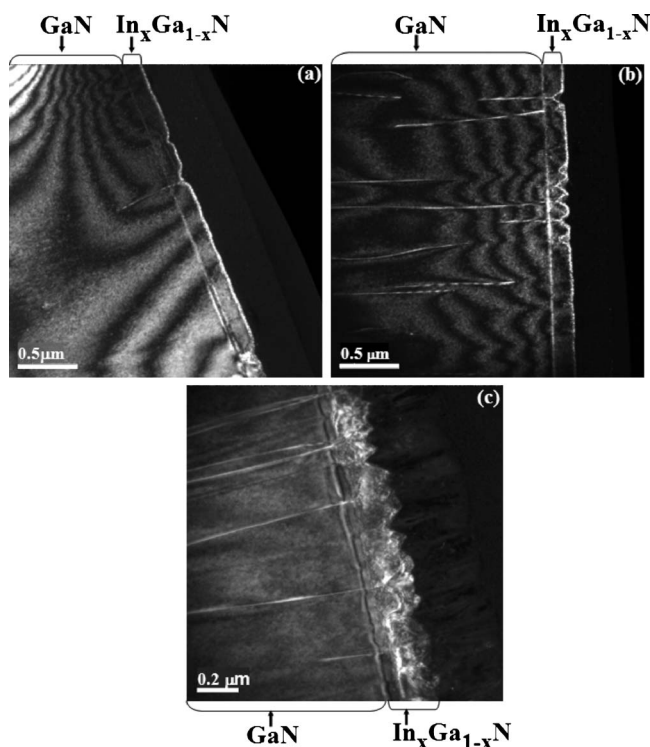


FIG. 2. Cross-sectional weak beam TEM images of (a) $\text{In}_{0.07}\text{Ga}_{0.93}\text{N}$, (b) $\text{In}_{0.10}\text{Ga}_{0.90}\text{N}$, and (c) $\text{In}_{0.14}\text{Ga}_{0.86}\text{N}$, respectively. Some threading dislocations are visible in GaN while V-pits are distinctly visible in InGaN. The images are taken using diffraction vector $g=0002$.

$\text{In}_{0.14}\text{Ga}_{0.86}\text{N}$ contains the highest number of V-pits as compared to $\text{In}_{0.07}\text{Ga}_{0.93}\text{N}$ and $\text{In}_{0.10}\text{Ga}_{0.90}\text{N}$ specimen, as seen in the images.

Optical properties of the InGaN film like the refractive index are crucial for the development of optoelectronic devices. The optical indices of GaN and $\text{In}_x\text{Ga}_{1-x}\text{N}$ were obtained by an inversion technique, which is a method extensively used these days for the analysis of SE measurements.¹⁴ In brief, this technique uses a model developed at the University of Mons¹⁵ for the simulation of the optical properties of a stack of films deposited on a thick substrate. In this model,¹⁵ each material is characterized by its optical indices (n, k) which are estimated by a parametric dispersion law (e.g., Tauc–Lorentz) depending on the photon energy. A real sample is modeled by a stack of very thin films (having different constant optical indices) with a profile representing optical indices with depth. This profile can exhibit sharp steps due to the interface between different materials, or smooth variations due to a change in the microstructure of a layer (roughness, diffused interface, compactness variations, and dislocation density) (see Fig. S2 of Ref. 16). In this model, the optical indices profile also takes into account the voids profile in the layer. The indices of a mixture of compact material and voids are thereby obtained by using the Bruggeman effective medium approximation.¹⁷

By conducting SE measurements we obtain two parametric values, namely, Δ and Ψ (or derivatives of these values), which are functions of photon energy E and the angle of incidence. The inversion technique mentioned before fits the Δ and Ψ values obtained from the optical model (by using Tauc–Lorentz dispersion law) of the sample with the experimental values obtained by SE (see Fig. S1 of Ref. 16). The fit is obtained by using the Levenberg–Marquardt algorithm with a biased least-squares estimator.¹⁵ This combination allows to obtain a covariance matrix of the model parameters which gives a 90% confidence interval for these parameters.¹⁸ For more information concerning the SE fitting and Tauc–Lorentz parametric law, refer to the supporting information.

The GaN and $\text{In}_x\text{Ga}_{1-x}\text{N}$ /GaN samples were analyzed by using a suitable model for the microstructure and a Tauc–Lorentz dispersion law for the optical indices.¹⁹ In case of InGaN/GaN samples, the surface of InGaN was considered to be rough (consistent with SEM and AFM observations) as well as compactness variation was taken into account in the InGaN and GaN films. The best fit obtained for $\text{In}_{0.07}\text{Ga}_{0.93}\text{N}$ resulted in a $\chi^2=4.23$. The optical microstructure of (a) $\text{In}_{0.07}\text{Ga}_{0.93}\text{N}$, (b) $\text{In}_{0.10}\text{Ga}_{0.90}\text{N}$, and (c) $\text{In}_{0.14}\text{Ga}_{0.86}\text{N}$ obtained by fitting the SE data are shown in Fig. S3. The thickness of each layer obtained by using this model agrees quite well with the thicknesses observed in SEM. The optical indices extraction proved to be difficult due to the following facts: (1) microstructure of both InGaN and GaN layers had to be found; (2) the thickness of InGaN layers is very small (200 nm) compared to the GaN sublayer (2.2 μm); (3) optical indices of InGaN are very close to those of GaN at least in the visible region. Sanford *et al.*¹⁰ have obtained a refractive index value of ~ 2.36 for $\text{In}_x\text{Ga}_{1-x}\text{N}$ ($x=0$ to 0.07) samples at $\lambda=633$ nm.

The refractive index n and extinction coefficient k obtained for the GaN and InGaN samples are plotted together in Fig. 3. The errors in the values are ± 0.02 and ± 0.05 for n

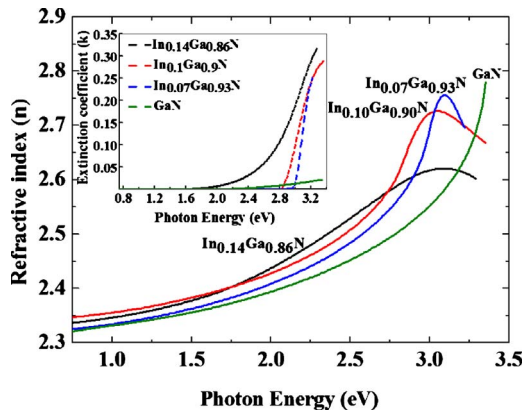


FIG. 3. (Color online) Calculated values of refractive index and extinction coefficient for GaN and $\text{In}_x\text{Ga}_{1-x}\text{N}$ ($x=0.07, 0.1, \text{ and } 0.14$) samples, obtained by using Tauc–Lorentz equation. Inset shows the extinction coefficient obtained for the three samples.

(GaN) and $n(\text{In}_x\text{Ga}_{1-x}\text{N})$ values, respectively, and ± 0.01 for k values (error bars not shown in the figure). These error values are obtained by covariance matrix method (90% confidence intervals). The line in green corresponds to GaN, blue to $\text{In}_{0.07}\text{Ga}_{0.93}\text{N}$, red to $\text{In}_{0.10}\text{Ga}_{0.90}\text{N}$, and black to $\text{In}_{0.14}\text{Ga}_{0.86}\text{N}$, respectively. The refractive index of GaN has been compared with values obtained on the same samples by a prism-coupling technique and close agreement has been found (results not shown here). The refractive index of $\text{In}_x\text{Ga}_{1-x}\text{N}$ are larger than GaN in the energy range 0.775 to 3.061 eV. The difference between $\text{In}_{0.1}\text{Ga}_{0.9}\text{N}$ and GaN is larger than 1.2%. Band gap related feature at ~ 3 eV is strongly pronounced in all the $\text{In}_x\text{Ga}_{1-x}\text{N}$ samples but is shifted to lower energies as compared to GaN. The gap structure is more broadened in case of $\text{In}_{0.14}\text{Ga}_{0.86}\text{N}$. This broadening can be possibly attributed to the increased alloy scattering and small compositional fluctuations as explained earlier by Goldhahn *et al.*¹¹ for their cubic $\text{In}_{0.02}\text{Ga}_{0.98}\text{N}$ and $\text{In}_{0.07}\text{Ga}_{0.93}\text{N}$ samples. A decrease in the refractive index of $\text{In}_{0.14}\text{Ga}_{0.86}\text{N}$ as compared to $\text{In}_{0.07}\text{Ga}_{0.93}\text{N}$, and $\text{In}_{0.10}\text{Ga}_{0.90}\text{N}$ is observed at the band gap structure which can be attributed to the inhomogeneity in the $\text{In}_{0.14}\text{Ga}_{0.86}\text{N}$ layer. The higher is the In composition, the higher will be the V-pits density (as seen in the TEM images and also from the Urbach tail for $\text{In}_{0.14}\text{Ga}_{0.86}\text{N}$ observed in the extinction coefficient spectra), resulting in a lower refractive index value.²⁰ The band gap structure is observed clearly in all the samples from the extinction coefficient curve shown in the inset in Fig. 3. The curves of $\text{In}_x\text{Ga}_{1-x}\text{N}$ samples shift to the lower energy side as the In composition x increases, resulting in a lower band gap energy. $\text{In}_{0.07}\text{Ga}_{0.93}\text{N}$ shows a sharp turning point at ~ 2.98 eV in the extinction curve while $\text{In}_{0.14}\text{Ga}_{0.86}\text{N}$ sample has the most broad damping stretched to around 1.77 eV (Urbach tail). The Urbach tail can be attributed to a number of mechanisms including the presence of point defects, disordered structure, excitonic transitions, or the presence of inhomogeneous strain in the semiconductor.²¹ This is in correspondence with the room temperature photoluminescence spectrum of $\text{In}_{0.14}\text{Ga}_{0.86}\text{N}$ layer which shows broad emission from ~ 1.77 to 3.02 eV (data not shown here).

In summary, structural and optical characterizations have been conducted for varying In content $\text{In}_x\text{Ga}_{1-x}\text{N}$ samples grown by MOCVD, with x varying up to 0.14. A model based on inversion technique was used to extract the refractive index and extinction coefficient by obtaining a best fit for the ellipsometric measurements. The thickness of each layer in InGaN samples obtained from the model could be directly correlated with the thickness obtained from SEM. The refractive index and extinction coefficient of $\text{In}_{0.14}\text{Ga}_{0.86}\text{N}$ were measured for the first time. This data is potentially important for the design of photonic devices using InGaN based materials.

This work was supported by funding from the CNRS and Nord Pas de Calais region in France and funding from A*STAR in Singapore as well as a grant awarded by the Embassy of France in Singapore through its Merlion program. Thanks to David Troadec (IEMN) for preparing samples by FIB for TEM measurements, Rayson Tan (IMRE) for conducting XRD measurements, and Dr. Debbie Seng (IMRE) for SIMS data acquisition.

- ¹F. K. Yam and Z. Hassan, *Superlattices Microstruct.* **43**, 1 (2008).
- ²S. Nakamura, M. Senoh, N. Iwasa, S. Nagahama, T. Yamada, and T. Mukai, *Jpn. J. Appl. Phys., Part 2* **34**, L1332 (1995).
- ³S. Nakamura and G. Fasol, *The Blue Laser Diode* (Springer, Berlin, 1997), pp. 201–260.
- ⁴J. Wu, W. Walukiewicz, K. M. Yu, W. Shan, J. W. Ager III, E. E. Haller, H. Lu, W. J. Schaff, W. K. Metzger, and S. Kurtz, *J. Appl. Phys.* **94**, 6477 (2003).
- ⁵K. Fujii, K. Kusakabe, and K. Ohkawa, *Jpn. J. Appl. Phys., Part 1* **44**, 7433 (2005).
- ⁶O. Khaselev and J. A. Turner, *Science* **280**, 425 (1998).
- ⁷K. Okamoto, J. Kashiwagi, T. Tanaka, and M. Kubota, *Appl. Phys. Lett.* **94**, 071105 (2009).
- ⁸T. Miyoshi, S. Masui, T. Okada, T. Yanamoto, T. Kozaki, S. Nagahama, and T. Mukai, *Appl. Phys. Express* **2**, 062201 (2009).
- ⁹M. Anani, H. Abid, Z. Chama, C. Mathieu, A. Sayede, and B. Khelifa, *Microelectron. J.* **38**, 262 (2007).
- ¹⁰N. A. Sanford, A. Munkholm, M. Krames, A. Shapiro, I. Levin, A. Davydov, S. Sayan, L. Wielunski, and T. Madey, *Phys. Status Solidi C* **2**, 2783 (2005).
- ¹¹R. Goldhahn, J. Scheiner, S. Shokhovets, T. Frey, U. Kohler, D. J. As, and K. Lischka, *Appl. Phys. Lett.* **76**, 291 (2000).
- ¹²C. Soh, W. Liu, J. Teng, S. Chow, S. Ang, and S. Chua, *Appl. Phys. Lett.* **92**, 261909 (2008).
- ¹³R. Liu, J. Mei, S. Srinivasan, H. Omiya, F. A. Ponce, D. Cherns, Y. Narukawa, and T. Mukai, *Jpn. J. Appl. Phys.* **45**, L549 (2006).
- ¹⁴G. E. Jellison, Jr., *Thin Solid Films* **313–314**, 33 (1998).
- ¹⁵E. Dumont, B. Dugnoille, and S. Bienfait, *Thin Solid Films* **353**, 93 (1999).
- ¹⁶See supplementary material at <http://dx.doi.org/10.1063/1.3425761> for the spectra showing the fitting pertaining to Δ and Ψ values and sample profile representing variation in optical indices with depth.
- ¹⁷P. J. Rouseel, J. Vanhellefont, and H. E. Maes, *Thin Solid Films* **234**, 423 (1993).
- ¹⁸C. M. Herzinger, P. G. Snyder, B. Johs, and J. A. Woollam, *J. Appl. Phys.* **77**, 1715 (1995).
- ¹⁹G. E. Jellison, Jr. and F. A. Modine, *Appl. Phys. Lett.* **69**, 371 (1996); **69**, 2137 (1996).
- ²⁰F. Natali, F. Semond, J. Massies, D. Byrne, S. Laugt, O. Tottereau, P. Vennegues, E. Dogheche, and E. Dumont, *Appl. Phys. Lett.* **82**, 1386 (2003).
- ²¹A. Cremades, L. Gorgens, O. Ambacher, M. Stutzmann, and F. Scholz, *Phys. Rev. B* **61**, 2812 (2000).